

Zn(II) coordination influences the secondary structure, but not antimicrobial activity of the N-terminal histatin 3 hydrolysis product

Emilia Dzień,^a Joanna Wątył,*^a Aleksandra Hecel,^a Aleksandra Mikołajczyk,^b Agnieszka Matera-Witkiewicz,^b Miquel Adrover,^{c,d,e} Miquel Barceló-Oliver,^c Alicia Domínguez-Martín*^f and Magdalena Rowińska-Żyrek*^a

^a Faculty of Chemistry, University of Wrocław, F. Joliot-Curie 14, 50-383 Wrocław, Poland

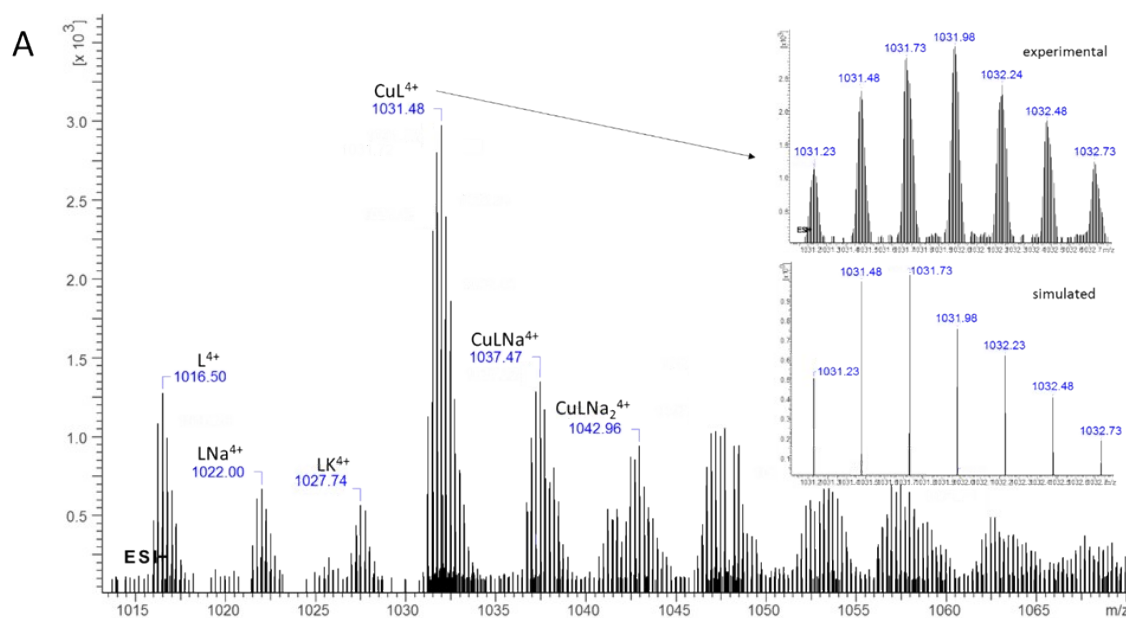
^b Screening of Biological Activity Assays and Collection of Biological Material Laboratory, Wrocław Medical University Biobank, Faculty of Pharmacy, Wrocław Medical University, Borowska 211A, 50-556 Wrocław, Poland

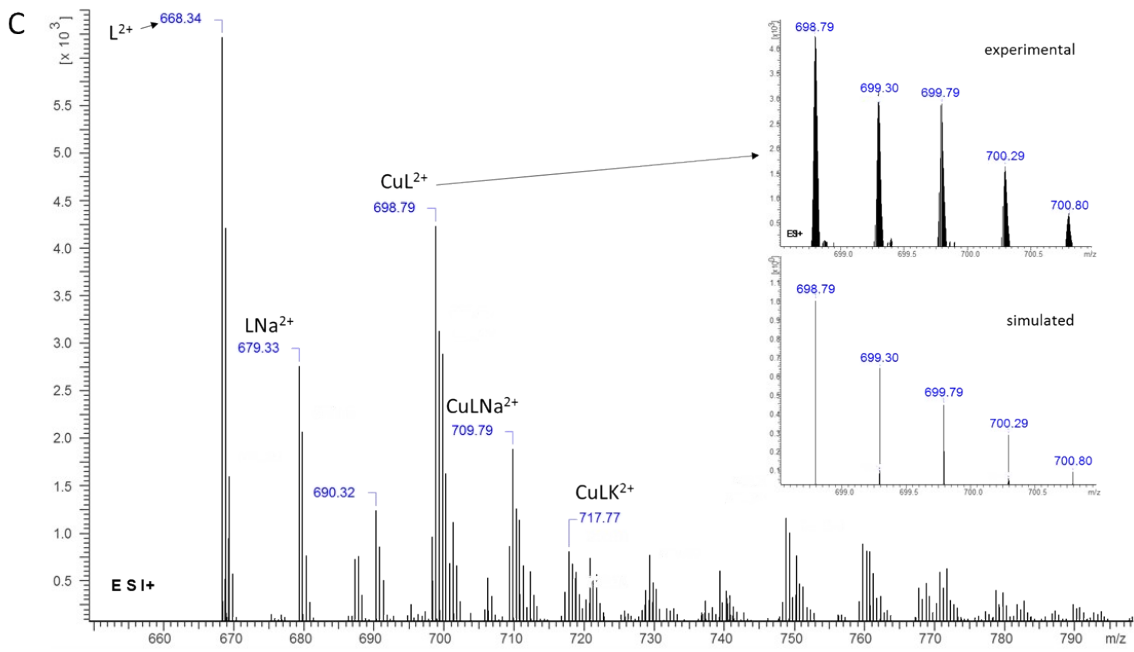
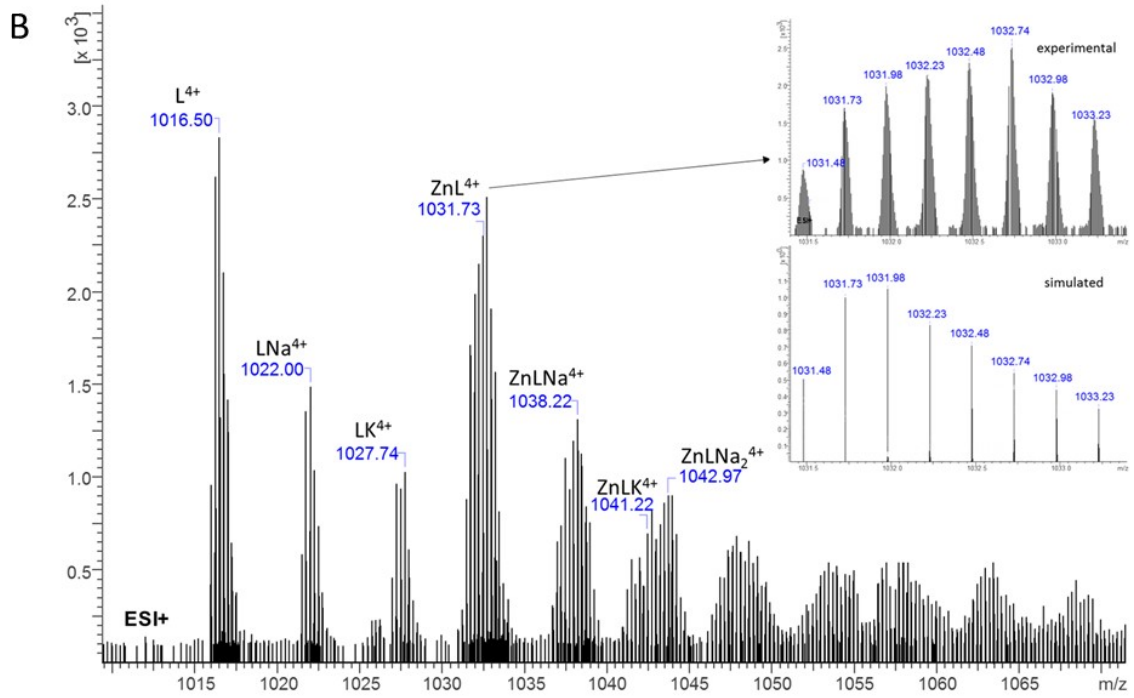
^c Department of Chemistry, University of Balearic Islands, Cra. de Valldemossa, km 7.7, 07122 Palma de Mallorca, Spain

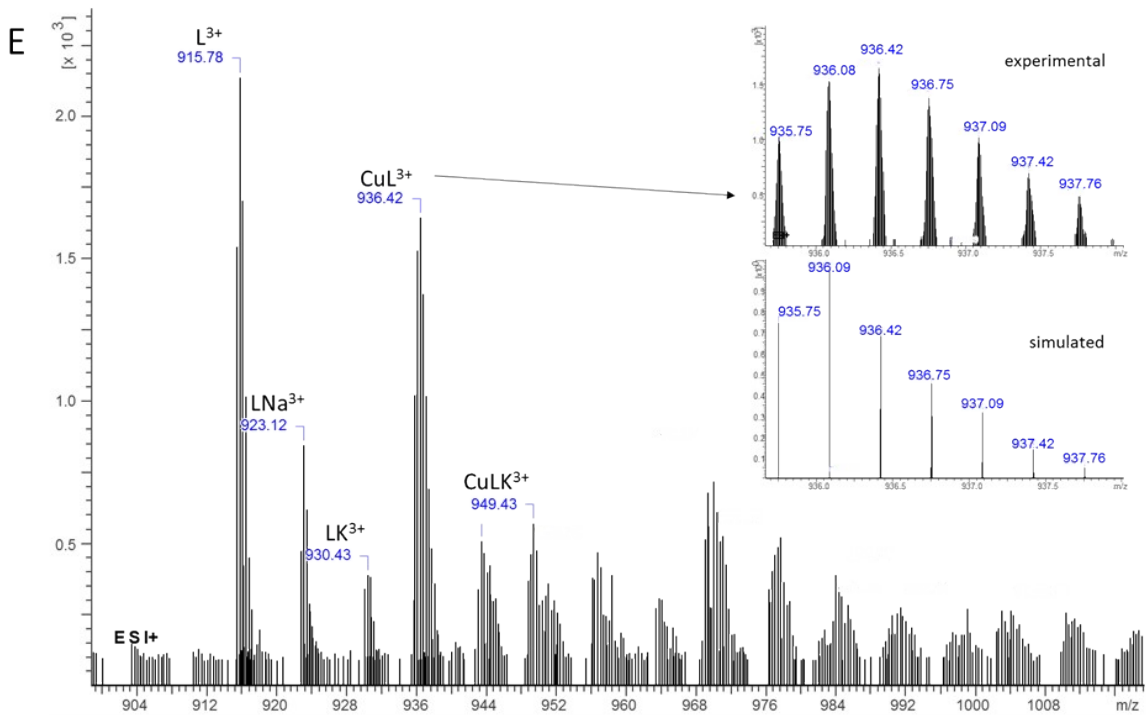
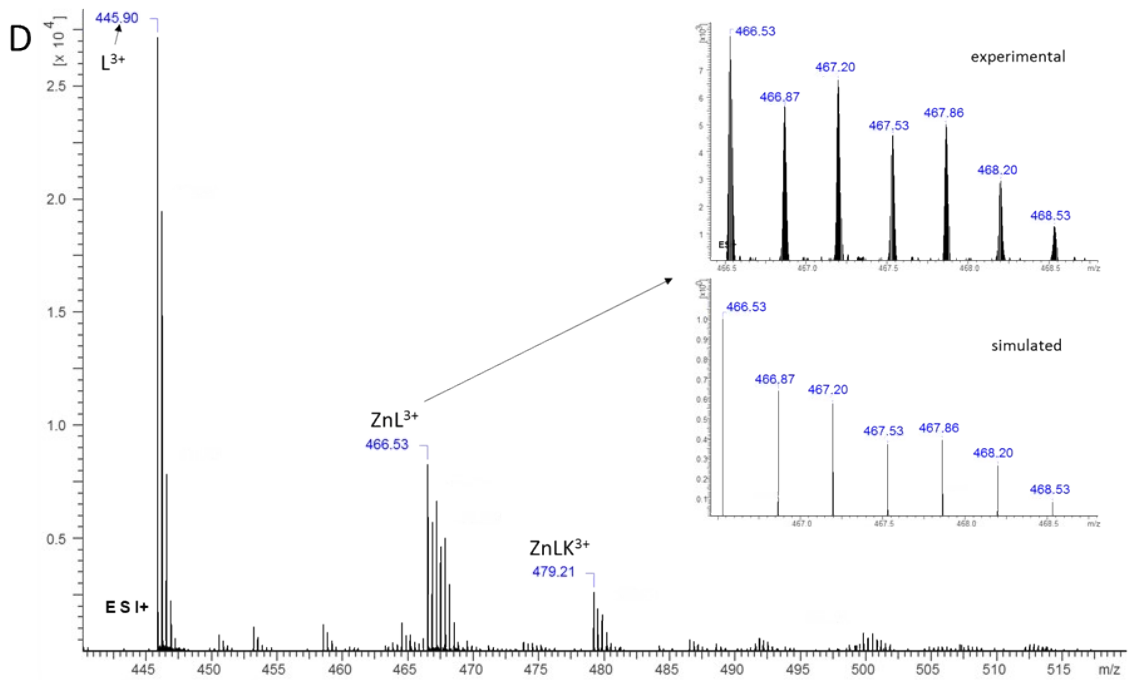
^d Institut Universitari d'Investigació en Ciències de la Salut (IUNICS),

^e Institut de Recerca en Ciències de la Salut (IdISBa),

^f Department of Inorganic Chemistry, Faculty of Pharmacy, University of Granada, E-18071 Granada, Spain







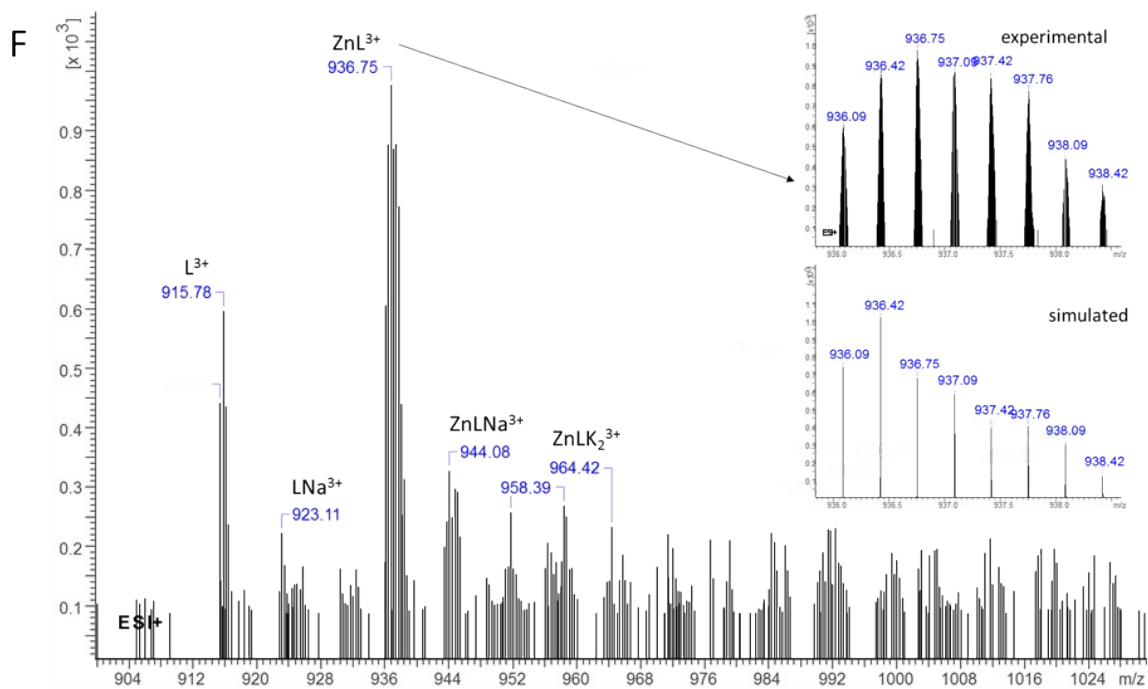
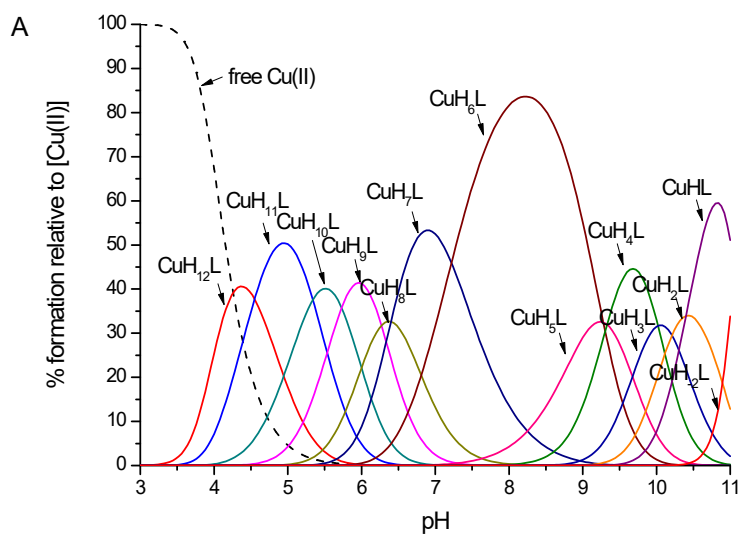


Fig. S1. ESI-MS spectra of: A) Cu(II)-histatin 3; B) Zn(II)-histatin 3; C) Cu(II)-histatin 3-4; D) Zn(II)-histatin 3-4; E) Cu(II)-histatin 4; F) Zn(II)-histatin 4; M:L molar ratio = 1:1, pH = 7.4 for Cu(II) complexes and pH = 8.0 for Zn(II) complexes.



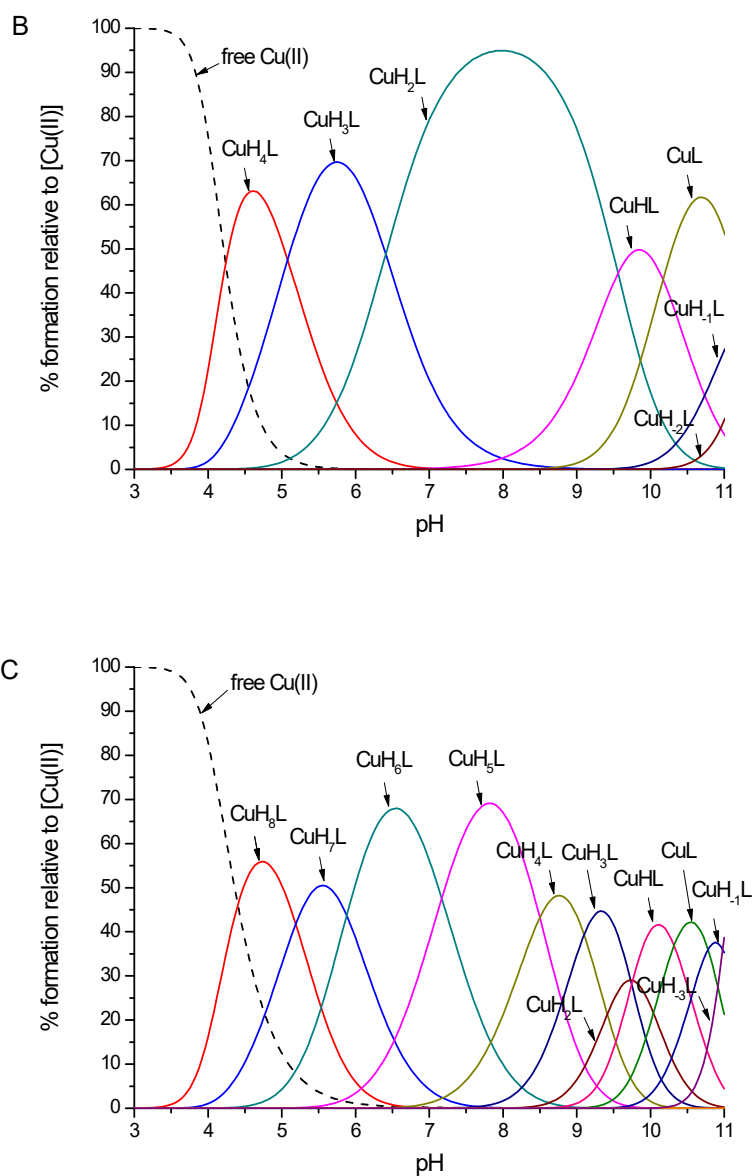
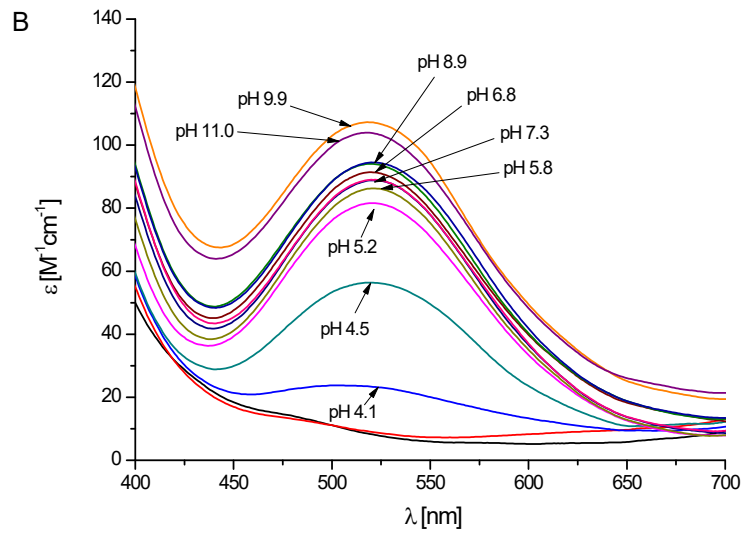
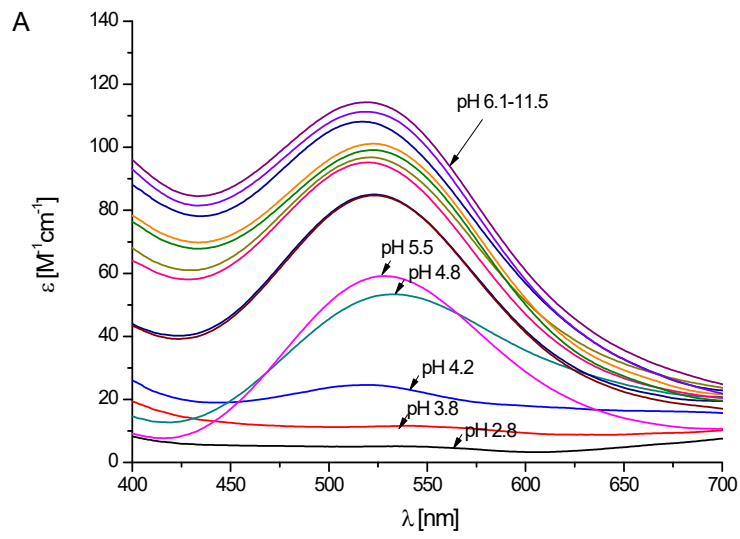


Fig. S2. Distribution diagrams for the formation of: A) Cu(II) complex with histatin 3; B) Cu(II) complex with histatin 3-4; C) Cu(II) complex with histatin 4. Conditions: $T = 298 \text{ K}$, $I = 0.1 \text{ M NaClO}_4$, $[\text{Cu(II)}] = 0.4 \times 10^{-3} \text{ M}$; M:L molar ratio = 0.8:1.



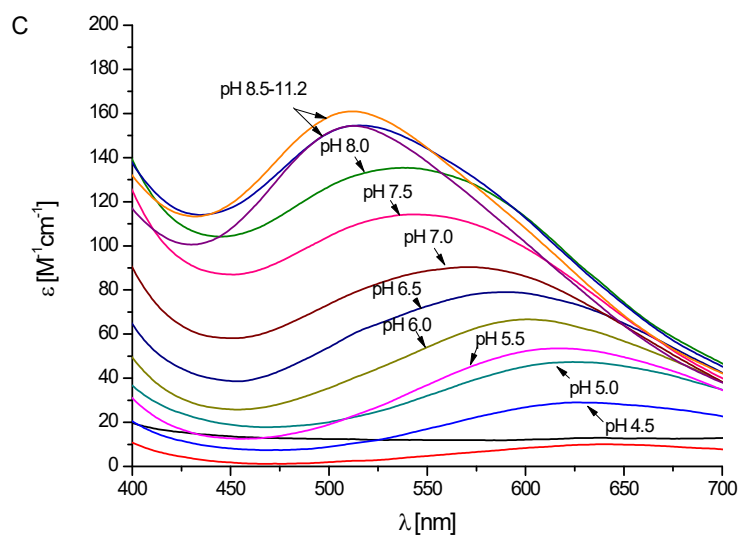
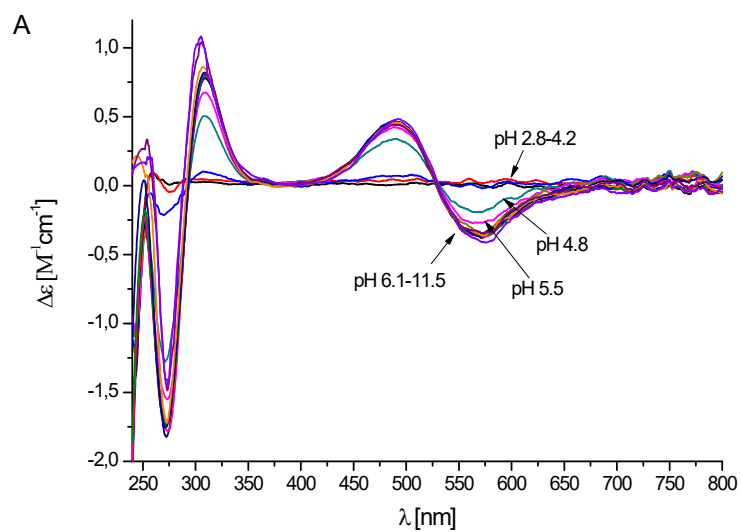


Fig. S3. UV-Vis spectra of Cu(II) complexes with: A) histatin 3; B) histatin 3-4; C) histatin 4; in pH range 2-11. Conditions: $T = 298 \text{ K}$, $I = 0.1 \text{ M NaClO}_4$, $[\text{Cu(II)}] = 0.4 \cdot 10^{-3} \text{ M}$; M:L molar ratio = 0.8:1.



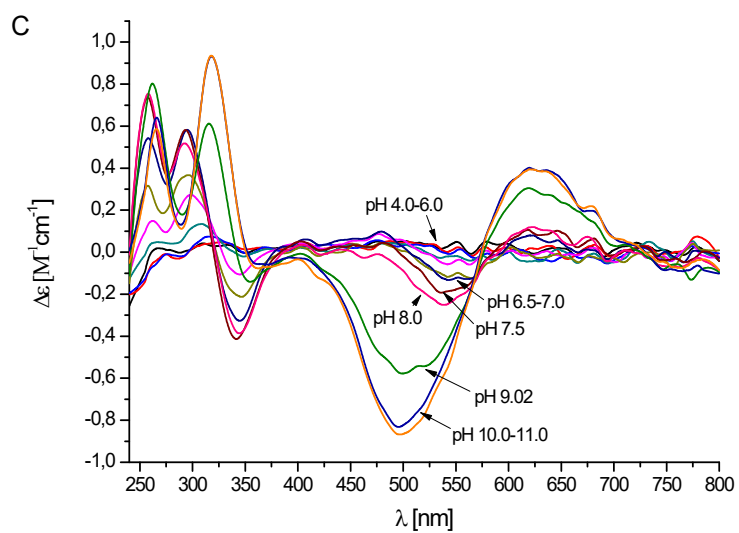
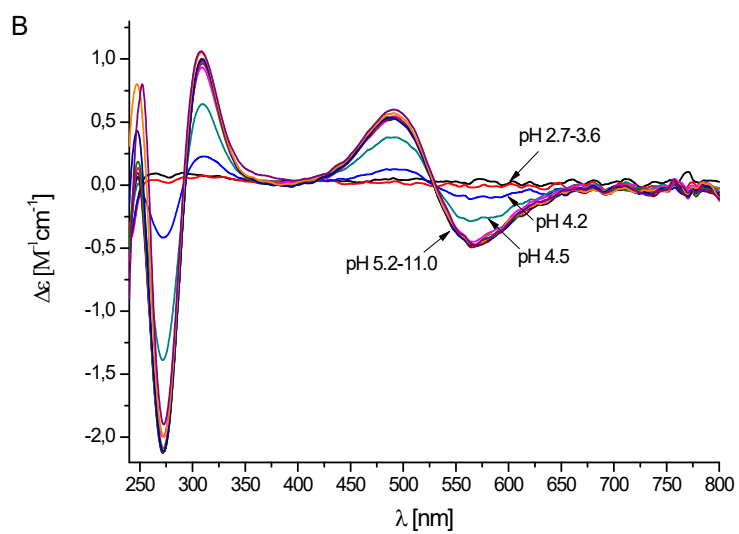


Fig. S4. CD spectra of Cu(II) complexes with: A) histatin 3; B) histatin 3-4; C) histatin 4; in pH range 2-11. Conditions: $T = 298 \text{ K}$, $I = 0.1 \text{ M NaClO}_4$, $[\text{Cu(II)}] = 0.4 \cdot 10^{-3} \text{ M}$; M:L molar ratio = 0.8:1.

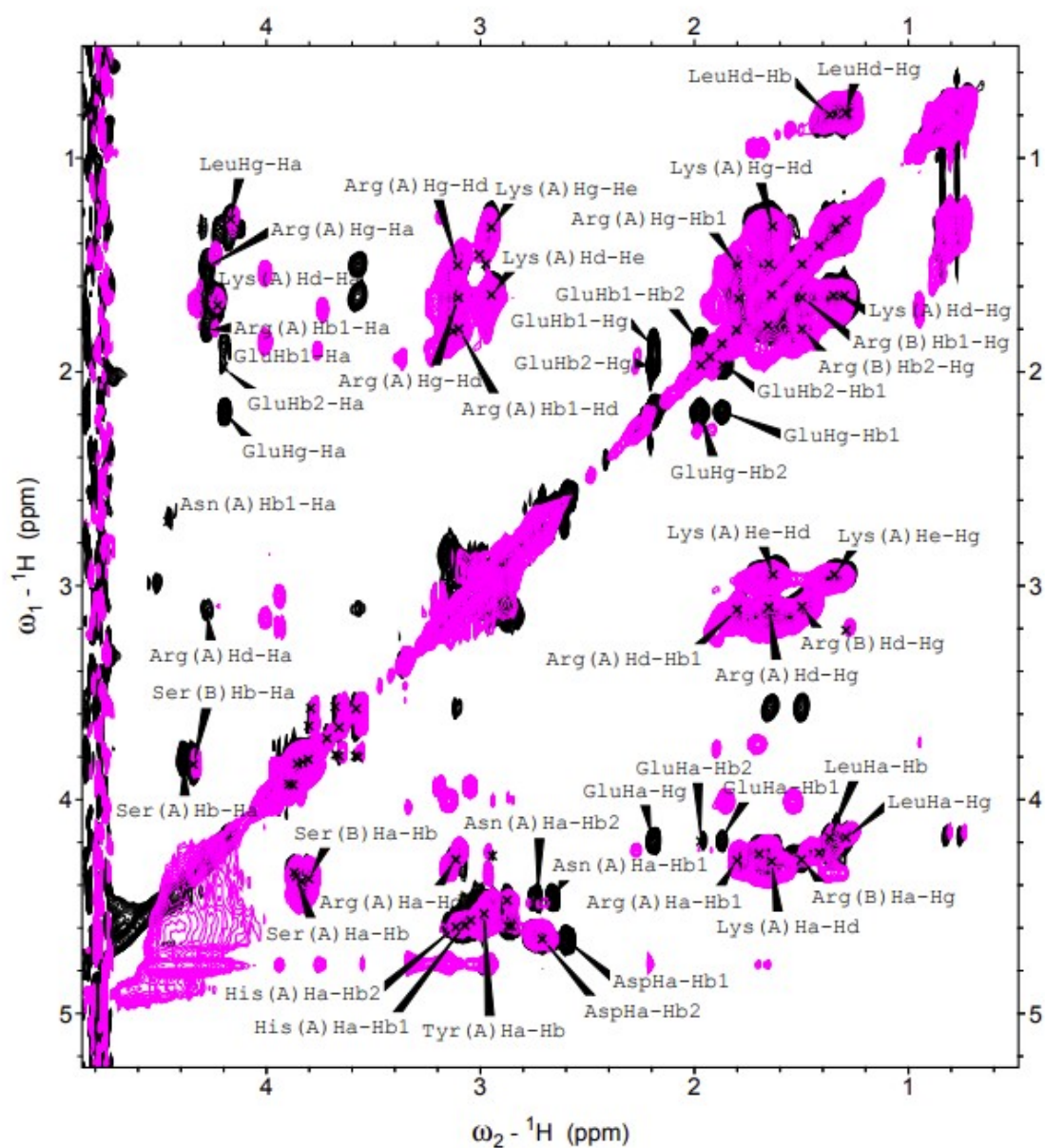
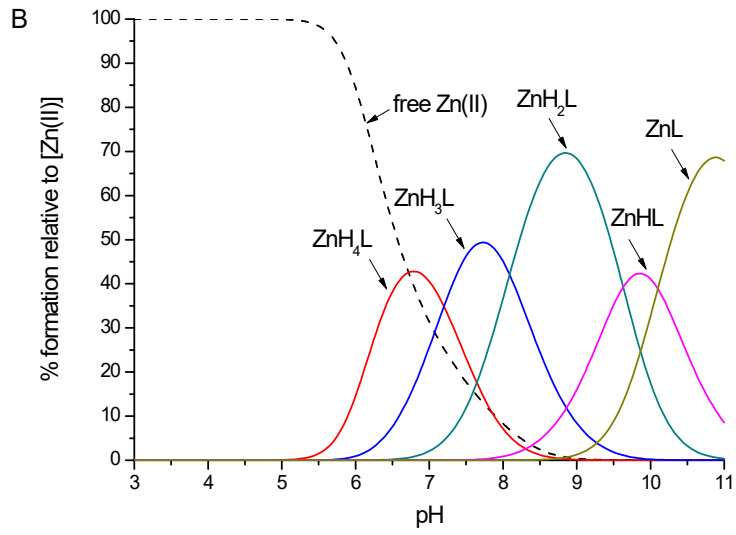
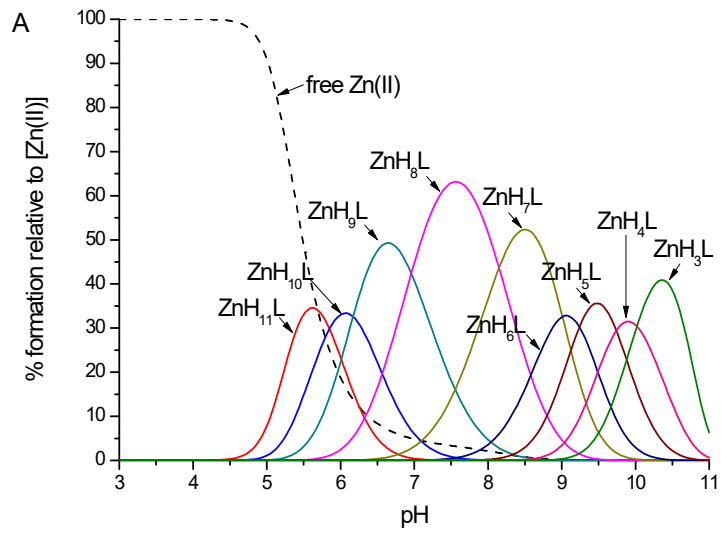


Fig. S5. ${}^1\text{H}$ - ${}^1\text{H}$ TOCSY NMR spectra of a fragment of the ligand (black) and the Cu(II) complex (pink) with the histatin 4, where (A) and (B) in the case of Ans, Arg, Lys, His, Ser and Tyr mean amino acid residues present in histatin 4, but without indicating a specific position in the peptide chain. Conditions: [histatin 4] = 1 mM, [Cu(II)] = 0.3 mM, pH = 7.4, T = 298 K.



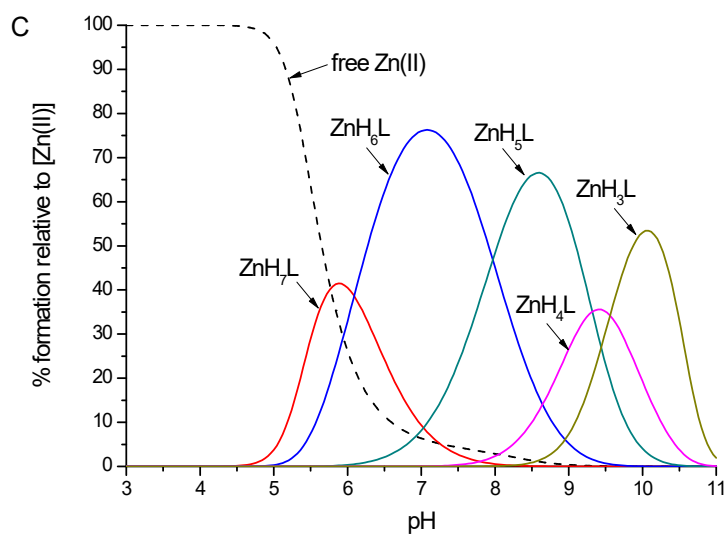
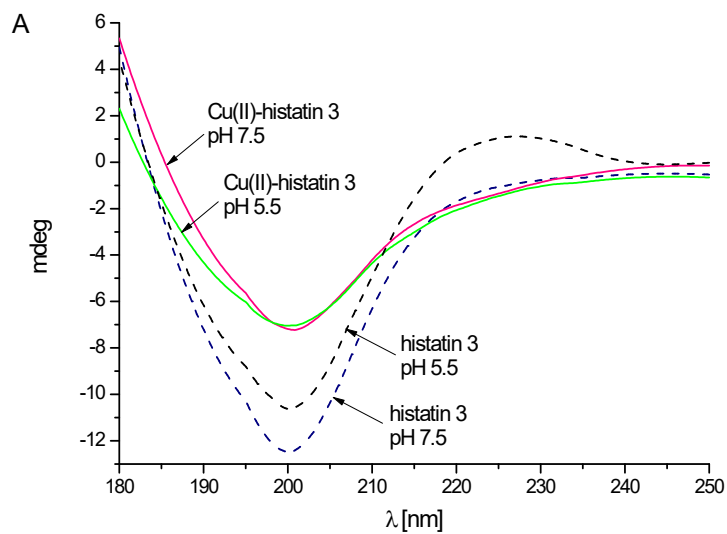
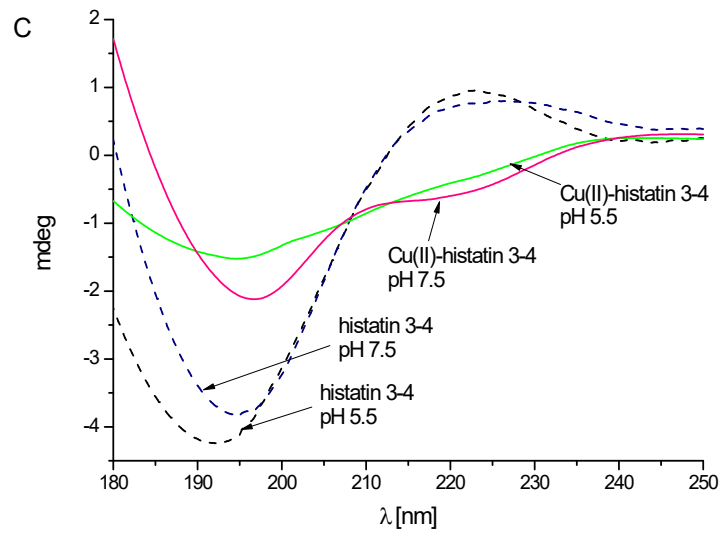
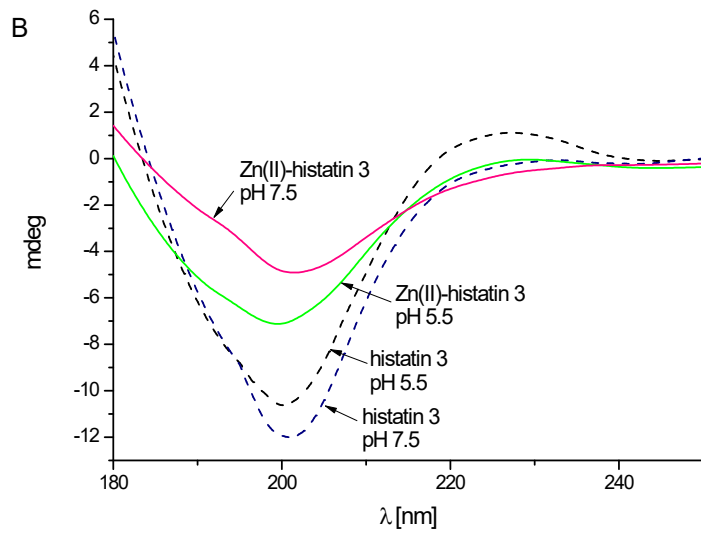


Fig. S6. Distribution diagrams for the formation of: A) Zn(II) complex with histatin 3; B) Zn(II) complex with histatin 3-4; C) Zn(II) complex with histatin 4. Conditions: $T = 298 \text{ K}$, $I = 0.1 \text{ M NaClO}_4$, $[\text{Zn(II)}] = 0.4 \times 10^{-3} \text{ M}$; M:L molar ratio = 0.8:1.





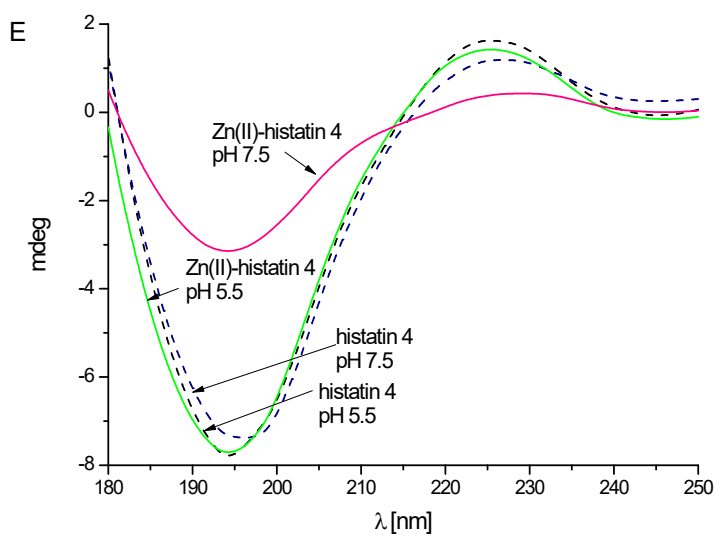
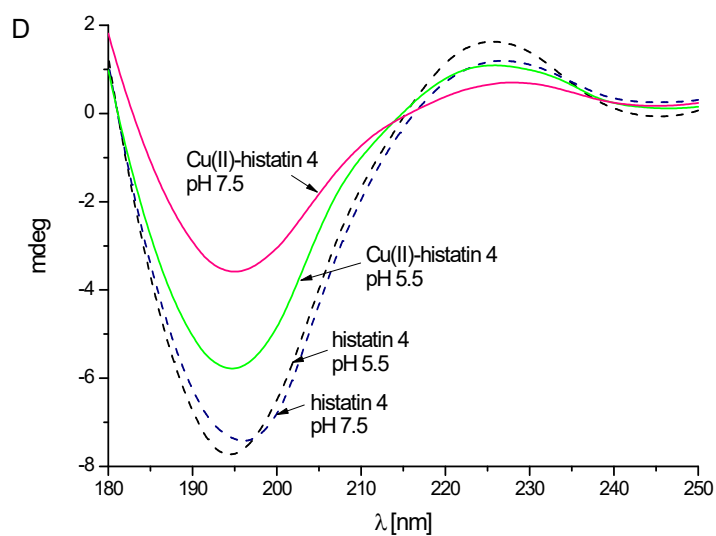


Fig. S7. Comparison of CD spectra of (A) histatin 3 and its Cu(II) complex, (B) histatin 3 and its Zn(II) complex, (C) histatin 3-4 and its Cu(II) complex, (D) histatin 4 and its Cu(II) complex and (E) histatin 4 and its Zn(II) complex at pH 5.5 and 7.5. Conditions: $T = 298 \text{ K}$, $I = 0.1 \text{ M NaClO}_4$, $[\text{Cu(II)}] = [\text{Zn(II)}] = 0.4 \cdot 10^{-3} \text{ M}$; M:L molar ratio = 0.8:1, optical path = 0.01 cm.

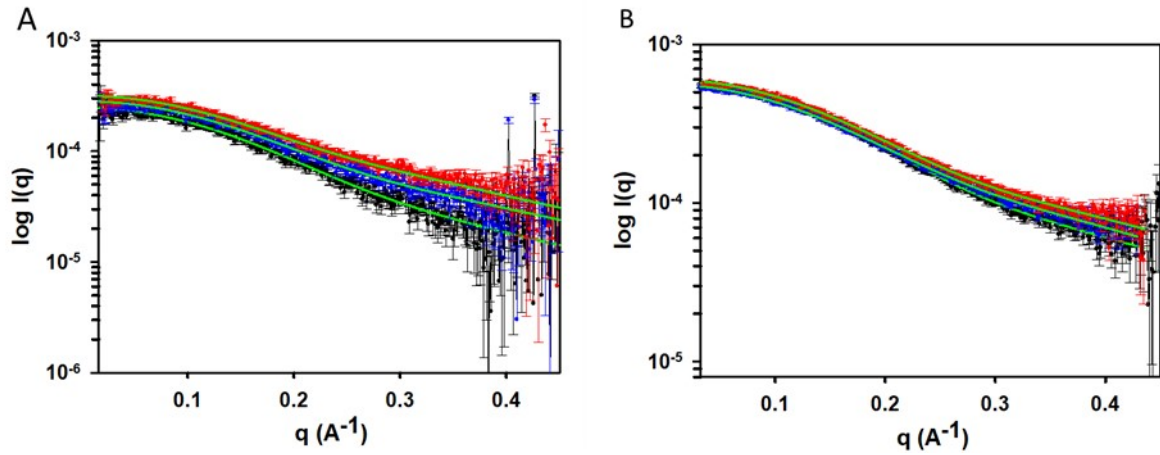


Fig. S8. The plots show the log of the scattering intensity (I , arbitrary units [a.u.]) as a function of momentum transfer ($q = 4\pi\sin(\theta)/\lambda$) for (A) histatin 3-4 and (B) histatin 5-8 obtained in the absence (black) and in the presence of Zn(II) at a Zn(II):peptide ratio of 1:1 (blue) and at 1.5:1 (red). The scattering curves were obtained setting the sample/detector distance at 630 mm. The line green line in the plots of panel B represents the GNOM fit.

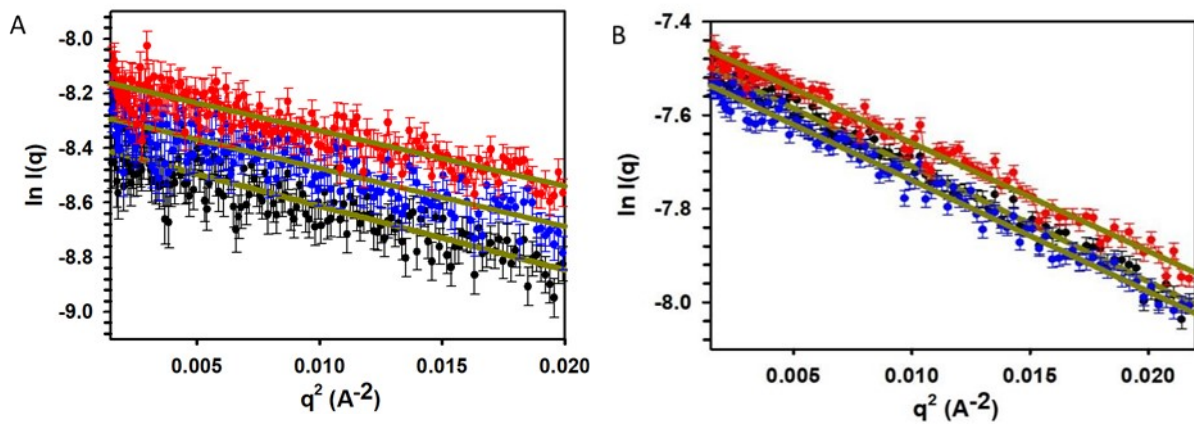


Fig. S9. Guinier plots of the SAXS curves corresponding to the low q region of (A) histatin 3-4 and (B) histatin 5-8 in the absence (black) and in the presence of Zn(II) at a Zn(II):peptide ratio of 1:1 (blue) and at 1.5:1 (red). The Green lines represent the fitting of the experimental data to the Guinier equation.

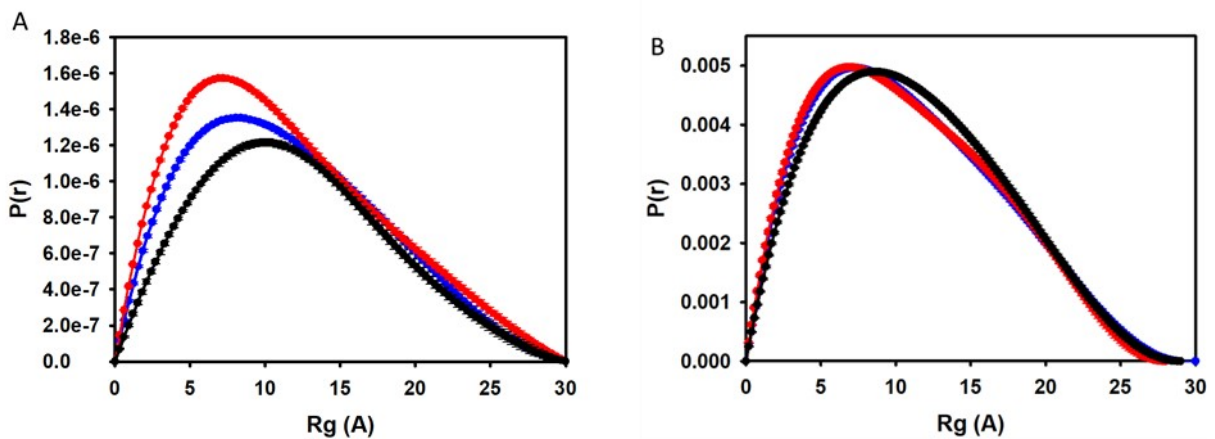


Fig. S10. Pair distance distribution functions of the scattering curve obtained for (A) histatin 3-4 and (B) histatin 5-8 in the absence (black) and in the presence of Zn(II) at a Zn(II):peptide ratio of 1:1 (blue) and 1.5:1 (red). The $P(r)$ values were determined using scattering data collected with the 0.03-0.45 \AA^{-1} q range.

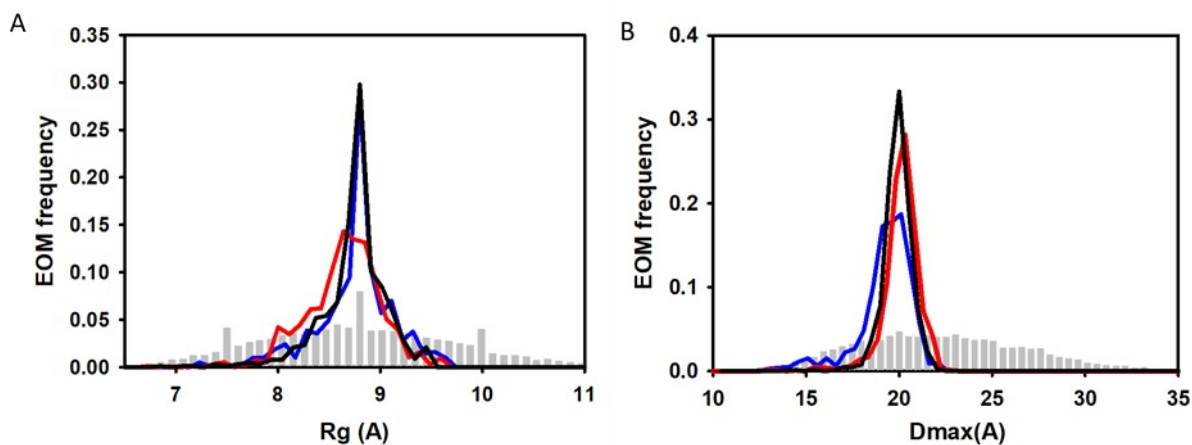


Fig. S11. SAXS analysis by Ensemble optimization method (EOM). Distribution of (A) R_g and (B) D_{max} values for the generated pool (grey bars) and the histatin 5-8 conformational ensemble (lines) obtained in the absence (black) and in the presence of Zn(II) at a Zn(II):peptide ratio of 1:1 (blue) and 1.5:1 (red).

Table S1. Examples of MIC breakpoints values from EUCAST/2023/06/29 for bacteria.¹

<i>Enterococcus</i> spp. (for <i>E. faecalis</i>)	MIC breakpoints ($\mu\text{g/mL}$)		<i>Staphylococcus</i> spp. (for <i>S. aureus</i>)	MIC breakpoints ($\mu\text{g/mL}$)		<i>Candida</i> spp. (for <i>C. albicans</i>)	MIC breakpoints ($\mu\text{g/mL}$)	
	S \leq	R $>$		S \leq	R $>$		S \leq	R $>$
Ampicillin	4	8	Azithromycin	2	2	Amphotericin B	1	1
Ampicillin-Sulbactam	4	8	Ceftobiprole	2	2	Fluconazole	2	4
-Amoxicillin	4	8	Ciprofloxacin	0.001	1	Micafungin	0.16	0.16
Amoxicillin-clavulanic acid	4	8	Daptomycin	1	1	Itraconazole	0.06	0.06
Imipenem	0.001	4	Maxifloxacin	0.25	0.25			
Ciprofloxacin	4	4	Amikacin	16	16			
Levofloxacin	4	4	Gentamicin	2	2			
Vancomycin	4	4	Tobramycin	2	2			
Linezolid	4	4	Teicoplanin	2	2			
Nitrofurantoin	64	64	Clindamycin	0.25	0.25			

References:

1. The European Committee on Antimicrobial Susceptibility Testing. Breakpoint tables for interpretation of MICs and zone diameters. Version 14.0, 2024. <http://www.eucast.org>.